

Magnetic order and spin fluctuations in the spin liquid $\text{Tb}_2\text{Sn}_2\text{O}_7$.

I. Mirebeau¹, A. Apetrei¹, J. Rodríguez-Carvajal¹, P. Bonville², A. Forget²,
D. Colson², V. Glazkov³, J. P. Sanchez³, O. Isnard^{4,5} and E. Suard⁵.

¹Laboratoire Léon Brillouin, CEA-CNRS, CE-Saclay, 91191 Gif-sur-Yvette, France.

²Service de Physique de l'Etat Condensé, CEA-CNRS, CE-Saclay, 91191 Gif-Sur-Yvette, France.

³Service de Physique Statistique, Magnétisme et Supraconductivité, CEA-Grenoble, 38054 Grenoble, France.

⁴Laboratoire de Cristallographie, Univ. J. Fourier-CNRS, BP 166, 38042 Grenoble France. and

⁵Institut Laüe Langevin, 6 rue Jules Horowitz, BP 156X, 38042 Grenoble France.

We have studied the spin liquid $\text{Tb}_2\text{Sn}_2\text{O}_7$ by neutron diffraction and specific heat measurements. Below about 2 K, the magnetic correlations change from antiferromagnetic to ferromagnetic. Magnetic order settles in two steps, with a smeared transition at 1.3(1) K then an abrupt transition at 0.87(2) K. A new magnetic structure is observed, not predicted by current models, with both ferromagnetic and antiferromagnetic character. It suggests that the spin liquid degeneracy is lifted by dipolar interactions combined with a finite anisotropy along $\langle 111 \rangle$ axes. In the ground state, the Tb^{3+} ordered moment is reduced with respect to the free ion moment ($9 \mu_B$). The moment value of $3.3(3) \mu_B$ deduced from the specific heat is much smaller than derived from neutron diffraction of $5.9(1) \mu_B$. This difference is interpreted by the persistence of slow collective magnetic fluctuations down to the lowest temperatures.

PACS numbers: 71.27.+a, 75.25.+z, 61.12.Ld

Geometrically frustrated pyrochlores $\text{R}_2\text{Ti}_2\text{O}_7$ show exotic magnetic behaviors^{1,2,3,4} such as dipolar spin ice (R=Dy, Ho) and spin liquid (Tb) phases, a first order transition in the spin dynamics (Yb), or complex antiferromagnetic orders (Er, Gd). The type of magnetic order depends on the balance between antiferromagnetic exchange, dipolar and crystal field energies^{5,6}. $\text{Tb}_2\text{Ti}_2\text{O}_7$ is a unique case of a spin liquid where short-ranged correlated magnetic moments fluctuate down to 70 mK, with typical energies 300 times lower than the energy scale given by the Curie-Weiss constant θ_{CW} of -19 K. The fact that $\text{Tb}_2\text{Ti}_2\text{O}_7$ does not order at ambient pressure², but could order under applied pressure, stress, and magnetic field^{7,8}, is still a challenge to theory, since recent models predict a transition towards antiferromagnetic (AF) long range order at about 1 K^{9,10}.

With respect to titanium, substitution by tin yields a lattice expansion. It also modifies the oxygen environment of the Tb^{3+} ion and therefore the crystal field. The stannates $\text{R}_2\text{Sn}_2\text{O}_7$ show the same crystal structure¹¹ as the titanates, and susceptibility data^{12,13} also suggest a great variety of magnetic behaviors. $\text{Dy}_2\text{Sn}_2\text{O}_7$ and $\text{Ho}_2\text{Sn}_2\text{O}_7$ are dipolar spin ices^{14,15} like their Ti parent compounds, whereas $\text{Er}_2\text{Sn}_2\text{O}_7$ does not order down to 0.15 K¹³, and $\text{Gd}_2\text{Sn}_2\text{O}_7$ undergoes a transition to AF order¹⁶. In $\text{Tb}_2\text{Sn}_2\text{O}_7$, magnetic measurements suggest an original and complex behavior. Antiferromagnetic interactions are observed at high temperature, yielding a Curie-Weiss constant θ_{CW} of -11 to -12 K^{12,13}, but a ferromagnetic (F) transition is seen around 0.87 K¹³.

We have performed neutron diffraction and specific heat measurements in $\text{Tb}_2\text{Sn}_2\text{O}_7$. With decreasing temperature a spin liquid phase is shown to transform into a new type of ordered phase, not predicted by theory, which could be called an "ordered spin ice". Just above the transition, an abnormal change in the spin correlations

shows the influence of dipolar interactions. By comparing the ordered Tb^{3+} moment values from neutron diffraction and nuclear specific heat, we also indirectly observe slow fluctuations of correlated spins, which persist down to the lowest temperature.

A powder sample of $\text{Tb}_2\text{Sn}_2\text{O}_7$ was synthesized. The crystal structure with space group $\text{Fd}\bar{3}m$ was studied at 300 K by combining X-ray diffraction with a neutron diffraction pattern measured in the diffractometer 3T2 of the Laboratoire Léon Brillouin (LLB). Rietveld refinements performed with Fullprof¹⁷ confirmed the structural model ($R_B=2.4\%$), yielding the lattice constant $a = 10.426 \text{ \AA}$ and oxygen position parameter $x=0.336$. The magnetic diffraction patterns were recorded between 1.4 K and 300 K and down to 0.1 K in the diffractometer G6-1 (LLB) and D1B of the Institut Laüe Langevin (ILL) respectively. The specific heat was measured by the dynamic adiabatic method down to 0.15 K.

Fig. 1 shows neutron diffraction patterns for several temperatures. The liquid-like peak corresponding to AF first neighbor correlations¹⁸ starts to grow below 100 K. Below 2 K, it narrows and slightly shifts and an intense magnetic signal appears at low q values. This shows the onset of ferromagnetic correlations, which progressively develop as the temperature decreases. Below 1.2 K, a magnetic contribution starts to appear on the Bragg peaks of the face centered cubic (fcc) lattice, which steeply increases at 0.87(2) K. This shows the onset of an ordered magnetic phase with a propagation vector $\mathbf{k}=0$.

Rietveld refinements of the magnetic diffraction patterns (Fig. 2) were performed with Fullprof¹⁷. The magnetic structure was solved by a systematic search, using the program BasIreps¹⁹ and symmetry-representation analysis²⁰. The basis states describing the Tb^{3+} magnetic moments were identified and the symmetry allowed structures were compared to experiment. Neither a

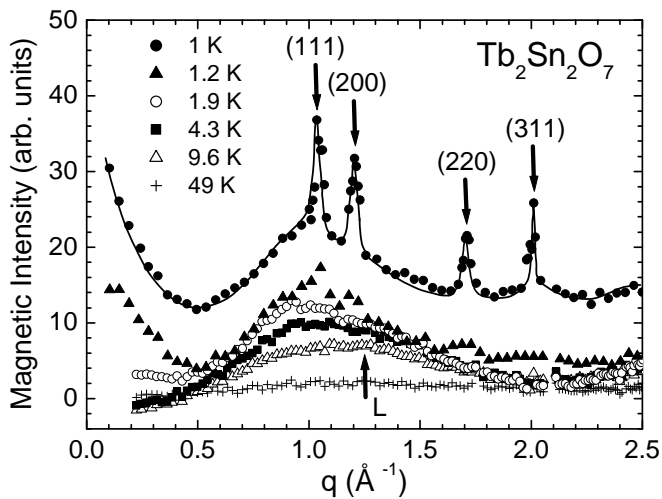


FIG. 1: Magnetic intensity of $\text{Tb}_2\text{Sn}_2\text{O}_7$ versus the scattering vector $q=4\pi\sin\theta/\lambda$. A spectrum in the paramagnetic phase (100 K) was subtracted. Intensities at 1. K have an offset of 10 for clarity. Arrows show the position of the Bragg peaks and near neighbor liquid peak (L) calculated in ref¹⁸

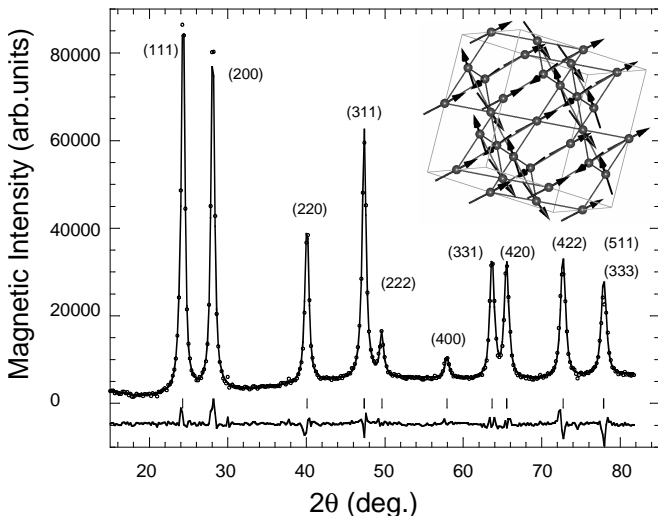


FIG. 2: Magnetic diffraction pattern of $\text{Tb}_2\text{Sn}_2\text{O}_7$ at 0.10 K versus the scattering angle 2θ . A spectrum at 1.2 K was subtracted. The neutron wavelength is 2.52 Å. Solid lines show the best refinement and the difference spectrum (bottom). In inset, the magnetic structure.

In the ordered structure with $\mathbf{k}=0$, the four tetrahedra of the cubic unit cell are equivalent. In a given tetrahe-

dron, the Tb^{3+} moments make an angle $\alpha=13.3^\circ$ with the local $\langle 111 \rangle$ anisotropy axes connecting the center to the vertices. The components along these $\langle 111 \rangle$ axes are oriented in the "two in, two out" configuration of the local spin-ice structure¹. The ferromagnetic component, which represents 37% of the Tb^{3+} ordered moment, orders in magnetic domains oriented along $\langle 100 \rangle$ axes. The perpendicular components make two couples of antiparallel vectors along $\langle 110 \rangle$ edge axes of the tetrahedron. The ordered moment ($M=5.9(1) \mu_B$ at 0.1 K) agrees with high field magnetization data ($5.5 \mu_B$ at 50 kOe and 2 K)¹³. It is reduced with respect to the free ion moment of $9 \mu_B$, as in $\text{Tb}_2\text{Ti}_2\text{O}_7$ ²⁹. With increasing temperature, M remains almost constant up to 0.6 K. Then it steeply decreases, showing an inflexion point which coincides with the T_c value of 0.87(2)K determined from the peaks in the specific heat and susceptibility¹³, and finally vanishes at 1.3(1)K (Fig. 3). The magnetic correlation length L_c was deduced from the intrinsic peak linewidth¹⁷. L_c remains constant and limited to about 190 Å up to T_c then starts to decrease above T_c . The angle α is constant within the experimental error.

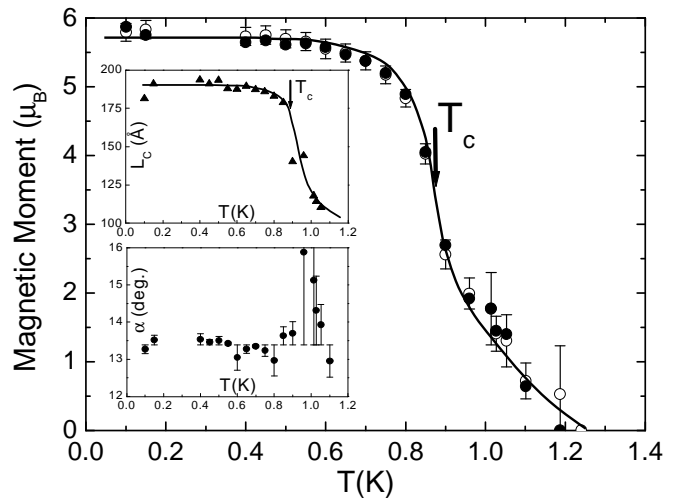


FIG. 3: Ordered magnetic moment M versus temperature (black circles) and squared intensity of the (200) magnetic peak, scaled to the moment at 0.10 K (open circles). T_c is determined from the peak in the specific heat. The correlation length L_c , deduced from the width of the magnetic Bragg peaks, and the angle α with the local anisotropy axis are plotted in the insets.

The magnetic ground state results from a delicate balance between exchange, dipolar and anisotropy energies. Several theories have been developed for specific cases involving the AF nearest neighbor exchange J_{nn} , the F nearest neighbor dipolar coupling D_{nn} and the strength of the local anisotropy D_a (all taken in absolute values). A spin liquid ground state is predicted for AF exchange only and Heisenberg spins²², namely for $J_{nn} \gg D_{nn}, D_a$. The dipolar spin ice state is stabilized for Ising spins when dipolar interactions overcome the AF exchange^{23,24}, namely for $D_a \gg D_{nn} > J_{nn}$. Its local

spin structure is similar to the observed one but spins keep the orientational disorder allowed by the "ice rules", whereas in $\text{Tb}_2\text{Sn}_2\text{O}_7$ they order to build a $\mathbf{k}=0$ structure. When either a finite anisotropy²⁵ ($J_{\text{nn}} \geq D_a \gg D_{\text{nn}}$) or a small dipolar coupling⁶ ($D_a \gg J_{\text{nn}} > D_{\text{nn}}$) are considered, a $\mathbf{k}=0$ structure is predicted, but the local order differs from the present one, since in a given tetrahedron all spins point either "in" or "out". Alternatively for Heisenberg spins when dipolar interactions dominate ($D_{\text{nn}} > J_{\text{nn}} \gg D_a$), a $\mathbf{k}=0$ structure is predicted, but the local spin structure consists of two couples of antiparallel moment oriented along the $\langle 110 \rangle$ edge axes of the tetrahedron²⁶. For an easy plane anisotropy ($D_a < 0$), the local order selected for the $\mathbf{k}=0$ structure, which is actually observed in $\text{Er}_2\text{Ti}_2\text{O}_7$, is also different⁴. The magnetic structure found in $\text{Tb}_2\text{Sn}_2\text{O}_7$ differs from all these ground states, and rather resembles the $\mathbf{k}=0$ structure of the dipolar spin ice $\text{Ho}_2\text{Ti}_2\text{O}_7$ in a low applied field¹. It may correspond to a case not considered above, where the three parameters have comparable magnitudes or obey the sequence $D_{\text{nn}} > D_a > J_{\text{nn}}$. Its ferromagnetic character suggests that the degeneracy of the spin liquid state which results from the AF near neighbor exchange is lifted by dipolar interactions, the strength of the uniaxial anisotropy tuning the angle α .

The unusual change with temperature in the short range correlations from AF to F type supports this interpretation. Somewhat similar effects occur in the partly itinerant LiV_2O_4 , or in weak ferromagnets with anisotropic interactions. Here the onset of ferromagnetic correlations just above the transition suggests that they come from long range dipolar interactions, with effective nearest neighbor ferromagnetic interaction²⁷.

Specific heat measurements provide new information on the magnetic order in $\text{Tb}_2\text{Sn}_2\text{O}_7$. The temperature dependence of the specific heat C_p is shown in Fig 4. In good agreement with neutron diffraction data, the specific heat C_p starts to increase below about 1.5 K then shows a well defined peak at 0.87 K. The final increase of C_p below 0.38 K is attributed to a nuclear Schottky peak, resulting mainly from the splitting of the energy levels of the ^{159}Tb nuclear spin ($I=3/2$) by the hyperfine field due to the Tb^{3+} electronic moment. This nuclear peak was observed down to 0.07 K in the parent compound $\text{Tb}_2\text{GaSbO}_7$ ²⁸.

site	x	y	z	M_x	M_y	M_z
1	0.5	0.5	0.5	3.85 (1)	3.85 (1)	2.20 (1)
2	0.25	0.25	0.5	-3.85 (1)	-3.85 (1)	2.20 (1)
3	0.25	0.5	0.25	3.85 (1)	-3.85 (1)	2.20 (1)
4	0.5	0.25	0.25	-3.85 (1)	3.85 (1)	2.20 (1)

TABLE I: Magnetic components M_x , M_y and M_z of the four Tb^{3+} moments (in μ_B) in one tetrahedron at 0.1 K. The atomic coordinates x , y , z , and the magnetic components are expressed in the cubic unit cell.

For $T < 0.38$ K, where the nuclear contribution is dominant, the full hyperfine hamiltonian, including a small estimated quadrupolar term, was diagonalized to obtain the four hyperfine energies. Then the standard expression for a Schottky anomaly was used to compute the nuclear specific heat C_{nuc} . The lines in Fig.4 below 0.8 K represent: $C_p = C_{\text{nuc}} + C_m$, where $C_m = \beta T^3$ is an empirical electronic magnon term which fits well the rise of C_p above 0.4 K, with $\beta = 12.5 \text{ J K}^{-4} \text{ mol}^{-1}$. The best fit to the data is obtained with a hyperfine field of 135 T, which corresponds to a Tb^{3+} moment value of $3.3(3) \mu_B$, using the hyperfine constant of $40(4) \text{ T}/\mu_B$. The electronic entropy variation S was computed by integrating $(C_p - C_{\text{nuc}})/T$ (inset of Fig.4). In $\text{Tb}_2\text{Sn}_2\text{O}_7$, our current measurements show that the crystal field level scheme is only slightly modified with respect to that in $\text{Tb}_2\text{Ti}_2\text{O}_7$, where the lowest states are two doublets separated by 18 K²⁹. Therefore S should reach the values $R \ln 2$ and $R \ln 4$ when T increases above T_c , as the first two doublets become populated. In fact, the entropy released at the transition is only 25% of $R \ln 2$, and it reaches 50% of $R \ln 2$ at 1.5 K. This reflects the strong correlations of the magnetic moments in the spin liquid phase above 1.5 K.

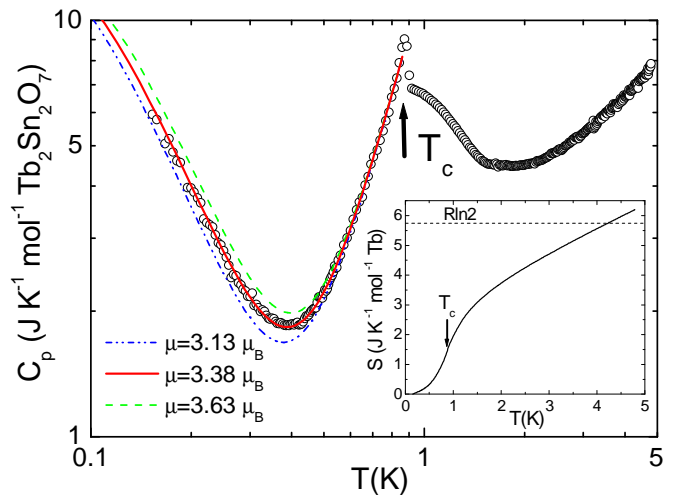


FIG. 4: Specific heat C_p in $\text{Tb}_2\text{Sn}_2\text{O}_7$. The curves below 0.8 K are the sum of a T^3 magnon contribution and of a nuclear Schottky anomaly, the latter being computed for 3 moment values (see text). The electronic entropy variation is shown in the inset. The arrows label the transition at $T_c = 0.87$ K.

The value $3.3(3) \mu_B$ for the Tb moment deduced from the nuclear specific heat is therefore well below the neutron value $5.9(1) \mu_B$. Such a remarkable reduction can be explained by the presence of electronic fluctuations. This happens if the characteristic time τ of these fluctuations becomes comparable to the spin-lattice nuclear relaxation time T_1 which governs the thermalization of the nuclear energy levels, as in $\text{Gd}_2\text{Sn}_2\text{O}_7$ ³⁰. Within the model³⁰, we find that a ratio $T_1/\tau = 0.4$ reduces the nuclear specific heat by a factor 2 and accounts for the neutron result. This implies low temperature fluctuations of the Tb^{3+} moments in the time scale 10^{-5} s,

much slower than for paramagnetic spins (10^{-11} s), which means that these fluctuations involve correlated spins, as previously noticed in geometrically frustrated magnets²³. Here, they occur in magnetically ordered domains and may be connected with their finite size. They could be probed by ^{119}Sn Mössbauer or muon spin relaxation experiments³⁰.

Why does $\text{Tb}_2\text{Sn}_2\text{O}_7$ order and not $\text{Tb}_2\text{Ti}_2\text{O}_7$? The weaker exchange energy in $\text{Tb}_2\text{Sn}_2\text{O}_7$ may not be the main reason. Our current crystal field study of the two compounds by high resolution neutron scattering suggests another possibility. In $\text{Tb}_2\text{Sn}_2\text{O}_7$ only, we have observed a small splitting (1.5 K) of a low energy excitation. It shows a lifting of the degeneracy of a crystal field doublet, possibly due to the higher value of the oxygen parameter which controls the local distortion around the Tb^{3+} ion. Assuming that the spectral density of the spin fluctuations decreases with energy, this lifting could weaken in $\text{Tb}_2\text{Sn}_2\text{O}_7$ the quantum fluctuations re-

sponsible for the persistence of the spin liquid state in $\text{Tb}_2\text{Ti}_2\text{O}_7$, and allow long range order to set in.

In conclusion, we observed a new magnetic structure in the spin liquid $\text{Tb}_2\text{Sn}_2\text{O}_7$. This unpredicted structure with both ferro and antiferromagnetic character could be called an 'ordered dipolar spin ice'. It arises below 1.3(1) K with a low ordered moment and strong fluctuations. Then at 0.87 K a steep increase of the ordered moment coincides with a peak in the specific heat. In the spin liquid phase, ferromagnetic correlations replace antiferromagnetic ones below about 2 K. In the ground state, the lower Tb^{3+} moment estimated from specific heat shows that the hyperfine levels are out of equilibrium and evidences the persistence of slow magnetic fluctuations of correlated spins. These unconventional fluctuations are reminiscent of the spin liquid in the ordered phase.

We thank F. Bourée for the neutron measurement on the diffractometer 3T2. We also thank F. Thomas and the cryogenic team of the ILL.

-
- ¹ M. J. Harris *et al.*, Phys. Rev. Lett. **79**, 2554 (1997).
² J. S. Gardner *et al.*, Phys. Rev. Lett. **82**, 1012 (1999).
³ J. A. Hodges *et al.*, Phys. Rev. Lett. **88**, 77204 (2002).
⁴ J. D. M. Champion *et al.*, Phys. Rev. B. **64**, 140407(R) (2001) and **68**, 020401(R) (2003).
⁵ R. Siddharthan *et al.*, Phys. Rev. Lett. **83**, 1854 (1999).
⁶ B. C. den Hertog and M. J. P. Gingras, Phys. Rev. Lett. **84**, 3430 (2000).
⁷ I. Mirebeau *et al.*, Nature **420**, 54 (2002).
⁸ I. Mirebeau, I. N. Goncharenko, G. Dhalleme and A. Revcolevschi, Phys. Rev. Lett. **93**, 187204 (2004).
⁹ Y. J. Kao *et al.*, Phys. Rev. B **68**, 172407 (2003).
¹⁰ M. Enjalran *et al.*, J. Phys. Condens. Matter. **16**, S673 (2004).
¹¹ B. J. Kennedy, B. A. Hunter and C. J. Howard, J. Solid. State Chem. **130**, 58 (1997).
¹² V. Bondah-Jagalu and S. T. Bramwell, Can. J. Phys. **79**, 1381 (2001).
¹³ K. Matsuhira *et al.*, J. Phys. Soc. Japan, **71**, 1576 (2002).
¹⁴ K. Matsuhira, H. Hinatsu, K. Tenya and T. Sakakibara, J. Phys. Condens. Matter. **12**, L649, (2000).
¹⁵ H. Kadowaki, Y. Ishii, K. Matsuhira and Y. Hinatsu, Phys. Rev. B **65**, 144421 (2002).
¹⁶ P. Bonville *et al.*, J. Phys. Condens. Matter. **15**, 7777 (2003).
¹⁷ J. Rodríguez-Carvajal, Physica B **192**, 55 (1993).
¹⁸ B. Canals and D. A. Garanin Can. J. of Phys. **79**, 1323 (2001).
¹⁹ J. Rodríguez-Carvajal, BasIreps, URL <ftp://ftp.cea.fr/pub/llb/divers/BasIreps>
²⁰ Y. A. Izyumov, V. E. Naish, R.P. Ozerov, Neutron diffraction on magnetic materials (Consultants Bureau, New York, 1991).
²¹ The magnetic structure is obtained for a state described as a linear combination of the two basis vectors of the irreducible representation Γ_7 . To obtain the list of irreducible representations and basis functions for the case $I4_1/amd$ and $\mathbf{k}=0$, one has to run the program BasIreps using the coordinates of Tb atoms (0,0.5,0.5), (0,0,0.5), (-0.25,0.25,0.25), (0.25,0.25,0.25).
²² J. N. Reimers, A. J. Berlinsky and A. C. Shi, Phys. Rev. B. **43**, 865 (1991).
²³ S.T. Bramwell *et al.*, Phys. Rev. Lett. **87**, 047205 (2001).
²⁴ S. T. Bramwell and M. J. P. Gingras, Science **294**, 149 (2001).
²⁵ R. Moessner, Phys. Rev. B **57**, R5587 (1998).
²⁶ S. E. Palmer and J. T. Chalker, Phys. Rev. B. **62**, 488 (2000).
²⁷ R. G. Melko and M. J. P. Gingras J. Phys. Condens. Matter. **16**, R1277 (2004)
²⁸ H. W. J. Blöte, R.F. Wierlinga and W. J. Huiskamp, Physica **43**, 549 (1969).
²⁹ M. J. P. Gingras *et al.*, Phys. Rev. B **62**, 6496 (2000).
³⁰ E. Bertin *et al.* Eur. Phys. J. B. **27**, 347 (2002).